Shock and Vibration 11 (2004) 467–492
IOS Press

Dynamic behavior of a railway wheelset on a roller rig versus tangent track

N. Bosso, A. Gugliotta and A. Somà*
Mechanical Department, Politecnico of Torino, C.so Duca Abruzzi 24, 10129 Torino, Italy

In Memoria of Bruno:
"intellegi necesse est in ipsis rebus, quae discuntur et cognoscuntur, invitamenta inesse, quibus ad discendum cognoscendumnque moveamur (*Cicerone*)*"*

Received 28 May 2004

Abstract. This paper addresses the comparison of dynamic behavior of a wheelset on roller and on rails. The development of equations of kinematics and motion allow to put in evidence the intrinsic differences between the dynamic behavior on rail and on roller. The stylized conical profile approximation of the wheel allows to focus the attention on the differences in creepages definition and in contact point shift due to the roller curvature. The treatise is addressed to a full scale roller and can be extended in the case of scaled roller rig to be applied in the case of the test bench developed for experimental analysis. In the present paper numerical simulation and examples are used to proof the analytical results.

1. Introduction

The roller rig is an experimental device that has become, in recent years, an instrument for investigations in railway dynamics. The realization of a roller rig gives the opportunity to evaluate in a laboratory the running behavior of railway vehicles without the need of onerous tests on track. The track is simulated by rollers with a transversal profile corresponding to the real rail.

The roller rigs represent nowadays a widely used means for studies about railway dynamics. However, the reliability of the roller rig experimental results and its comparison with the behavior of a railway vehicle on a real track is still object of study. Other Authors have recently studied the problem using different approach [1–3].

Full size and scaled roller rigs are designed for different purposes. The former, expensive to be realized, are used to perform dynamic analyses on full sized railway vehicles. The scaled roller rigs, usually realized in a 1:5 scale, are used in order to perform dynamic analyses on models of single bogies. Main purpose of investigation performed on scaled Roller Rigs is the study of the wheel-rail contact phenomena and the validation of numerical codes. Direct applications in the pre-design phase of railway vehicles may be possible with the evaluation of the inherent errors due to the presence of roller instead of track.

The research group of the Politecnico of Torino is engaged in the realization of a scaled roller rig (1:5) developed with modular design concept [4]. The introduction of specific contact module has been developed [5]. The different scaling techniques are extensively compared and investigated by the authors [6].

In the present work mathematical models and computer programs are used in order to simulate the dynamic behavior of a wheelset running on rails and on rollers.

In such a way, the study proposes an approach for the comparison of the behavior of the wheelset in the two cases. These will be described in formulas and the influence on the dynamics of the systems can be relatively quantified.

*Corresponding author. E-mail: aurelio.soma@polito.it.

ISSN 1070-9622/04/$17.00

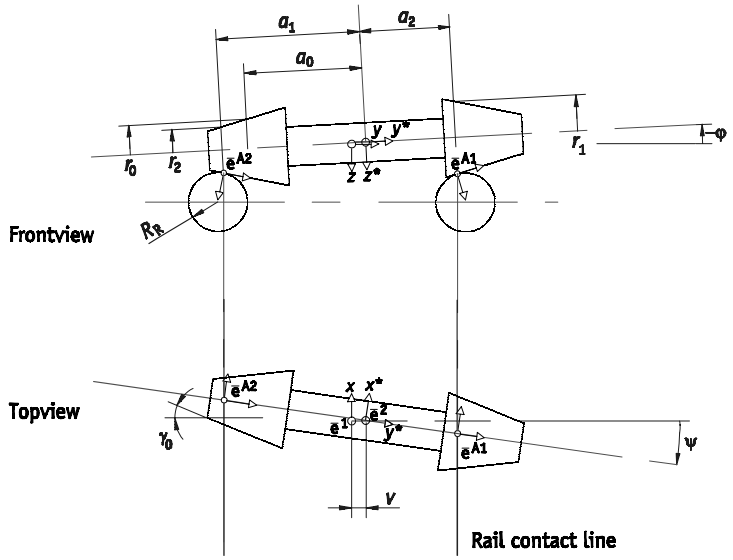

Fig. 1. wheelset on rails.

The study is focused on tangent track dynamics and actually limited to stylized profiles in order to allow an exhaustive analytical approach which evidences the differences between the two cases analyzed (roller rig versus track). This model is therefore mainly addressed to stability study, and is non suitable for curve dynamics where double point of contact due to flange occurs. For curving dynamics the adoption of real profile is important to achieve accurate results.

On the other hand actually it is not possible to investigate curving dynamics using a roller rig, due to high complexity of design and control system required to reproduce a realistic curved track using rollers.

In case of tangent track for stability, the model is able to predict a realistic value of the critical speed, because flange contact occurs only when the wheelset is already unstable, and its only effect is to limit the amplitude of the instability cycle.

2. Mathematical models

2.1. Description

With regards to the model of wheelset on rails, a simplified system composed by a dicone running on cylindrical rails is proposed (Fig. 1), according with the model proposed by Jaschinski in [3]. The model of wheelset on rollers is based on the scheme shown in Fig. 2 with the introduction of the curvature radius rr of the rollers. It is built with geometrical properties similar to those of the dicone on rails in order to compare the two models. It is evident that, in these two models, the nonlinearities due to the geometric contact are simplified. However, the systems still contain the nonlinearities due to friction. According to [3] and [7], the simplification assumed does not influence the fundamental behavior of the system and at the same time permits a clear interpretation of the peculiar characteristics of the systems and their comparison in analytical terms.

Some remarks about the notation used here and in the following are necessary:

- in the following, the index j will be used to indicate the side of the track; it is $j = 1$ for the right-hand side and $j = 2$ for the left-hand side.
- the symbol * indicates a variable defined in the body-fixed reference frame.

Some fundamental assumptions are now to be taken into account:

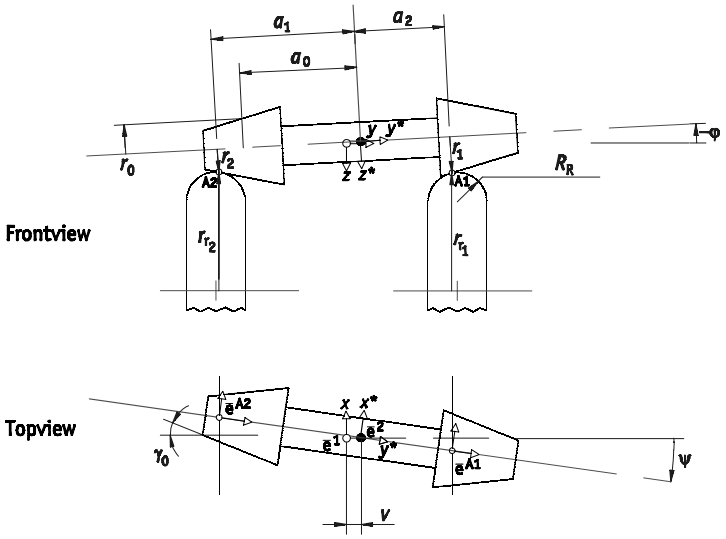

Fig. 2. wheelset on rollers.

- the center of mass of the wheelset running along the straight track translates with a constant nominal velocity V_n;
- the nominal spin angular velocity of the wheelset $\Omega_n = V_n/r_0$ is constant in both the systems (r_0 being the nominal rolling radius of the wheelset in the central position);
- the nominal spin angular velocity of the rollers $\Omega_r = V_n/r_r$ is constant (r_r being the nominal rolling radius of the roller with the wheelset in the central position);
- the wheelset is axisymmetric.

In Figs 1 and 2 the four fundamental reference frames considered are shown:

- the frame $\{o, \overline{e}^1\}$ is a track reference frame considering the wheelset on rails. It translates with constant velocity V_n along the tangent track center line. Considering the roller rig it becomes a fixed roller-body frame;
- the wheelset-body frame $\{o^*, \overline{e}^2\}$ has its origin located in the mass center of the wheelset and its axes coincide with the principal inertia axes of the body;
- the contact point frames $\{o^1, \overline{e}^{A1}\}$, $\{o^1, \overline{e}^{A2}\}$ have their origins located respectively in the right and left contact points A_1 and A_2.

2.2. *Contact constraints*

The wheelset is a rigid body and it is endowed with six degrees of freedom. The translational generalized coordinates are represented by the three displacements u, v, w (longitudinal, lateral, vertical) of the wheelset center of mass o^* with respect to o in the track reference frame. The rotational degrees of freedom, represented by the rotations about the axes o^*x^*, o^*y^*, o^*z^*, are respectively defined by the roll, spin and yaw angle: φ, ϑ, ψ.

In the mechanical system composed by the wheelset and the rails/rollers, only four generalized coordinates are independent. This is due to the fact that each wheel contacts the corresponding rail/roller in one point (only single point contact is considered in this work) and so there are two geometric contact constraints. It is known from [8] and [10] that the longitudinal displacement u and the spin rotation ϑ are uncoupled from the other degrees of freedom and have no influence on the geometric constraints, so they are considered to be independent generalized coordinates. Among the other four generalized coordinates, the lateral displacement y and the yaw rotation ψ are assumed to be independent.

According to [10] it is convenient to introduce an additional coordinate s representing the displacement of the track reference frame along the track and to replace the coordinate ϑ with the deviation of the nominal spin rotation χ, i.e., s and χ defined by the relations:

$$s = V_n t, \tag{1}$$

$$\chi = \frac{s}{r_0} - \vartheta, \tag{2}$$

The quantity χ can be considered of the same order of magnitude as the other generalized coordinates. Besides, when we call s^* the displacement of the wheelset-body frame, we have:

$$u = s^* - s. \tag{3}$$

The vector of the independent generalized coordinates reduces to:

$$\underline{q}^* = [u, v, \chi, \psi]^T. \tag{4}$$

The two constraint relations read:

$$\varphi = \varphi(v, \psi) \tag{5}$$

$$w = w(v, \psi). \tag{6}$$

An explicit form for these relations can be obtained by means of geometrical considerations. Jaschinski in [3] and De Pater in [11] obtain formulas that are valid for the case of a double cone on cylinders:

$$\varphi = -A_0 v \tag{7}$$

$$w = -\frac{1}{2} C_0 v^2 + \frac{1}{2} D_0 \psi^2 \tag{8}$$

where A_0, C_0, D_0, B_0 are the following geometrical parameters:

$$A_0 = \frac{\gamma_0}{a_0 - r_0 \gamma_0} \quad C_0 = A_0 + \frac{A_0^2}{B_0} \quad D_0 = \frac{\gamma_0^2}{A_0} \tag{9}$$

with $B_0 = \frac{\gamma_0}{a_0 + R_R \gamma_0}$.

Formulas Eqs (7–9) have been obtained with the assumption of small angles for ψ, φ and γ_0. In Eq. (7), according to [11], the effect of ψ yields a second order term that is negligible with respect to $A_0 v$.

2.3. Determination of the contact point locations

The determination of the location of the wheel-rail contact patches is necessary for both the application of the simplified rolling contact mechanics and for the definition of the equations of motion of the system. Because the axes of the contact ellipses are very small with respect to the dimensions of track-wheelset system, such as the nominal diameter of the wheels or the track gauge, the location of the contact patch can be determined considering it as the contact point originated by the contact of the two bodies postulating that they are perfectly rigid. The consequence of this assumption is that the determination of the position of the contact points and of the associated geometric parameters reduces to a pure geometrical problem.

For the determination of the actual rolling radii and of the contact point distances the formulas adopted from [3] will be used:

$$r_1 = r_0 + \lambda \nu \quad r_2 = r_0 - \lambda \nu \tag{10}$$

$$a_1 = a_0 - \lambda \frac{\nu}{\gamma_0} \quad a_2 = a_0 + \lambda \frac{\nu}{\gamma_0} \tag{11}$$

λ is a geometric parameter commonly called, in railway engineering, equivalent conicity:

$$\lambda = \frac{f(\text{rolling radius difference})}{\text{lateral displacement}}.$$

Mauer, in [9], proposed a formula for the calculation of λ:

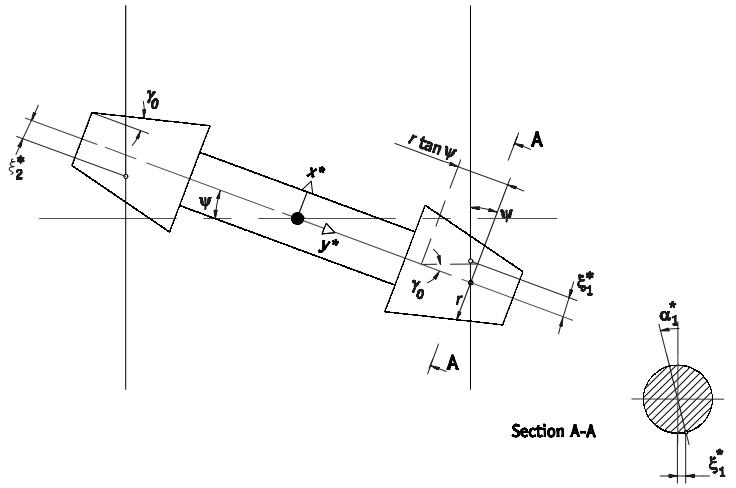

Fig. 3. Representation of the first order term of the contact point shift ξ^* and of the contact shift angle α^* for $\varphi = 0$ and $R_R = 0$.

$$\lambda = \frac{R_w \gamma_0}{R_w - R_R} \cdot \frac{a_0 + R_R \gamma_0}{a_0 - r_0 \gamma_0}. \tag{12}$$

Where R_R and R_w are respectively the rail and the wheelset curvature radii in the x-z plane.

In the particular case of a wheelset with conical profiles:

$$\lambda = a_0 A_0 + R_R \gamma_0 A_0. \tag{13}$$

Finally, in order to define the displacement of the contact points in the longitudinal direction it is necessary to introduce the contact point shift ξ. Even if the value of the parameter ξ is always very small, it is relevant because it has a direct influence on the direction of the constraint forces.

Due to the curvature of the rollers the definition of this variable becomes different when we pass from the wheelset on rails to the case of wheelset on rollers.

2.4. Wheelset on rails

It is convenient to consider the contact shift $\xi^* = \xi^*(\psi)$ defined in the wheelset-body frame. In the case of wheelset on rollers this shift is due uniquely to the yaw motion of the wheelset. The formulation of to be assumed in this case is the one given by [8] and [12]:

$$\xi_j^* = \pm r_0 \psi \gamma_0 - [r_0(a_0 + R_R \gamma_0)\gamma_0] \varphi \psi. \tag{14}$$

For small values of φ and ψ, the second order term can be neglected and so we obtain:

$$\xi_j^* = \pm r_0 \psi \gamma_0, \tag{15}$$

a formula obtained also by Jaschinski in [3] by means of geometrical considerations (Fig. 3).

If we consider the arc of the circular section of the dicone that corresponds to the contact point shift, we can also define the shift /angle shown in Fig. 3:

$$\alpha_j^* = \pm \frac{|\xi_j^*|}{r_j} = \pm \gamma_0 \psi \tag{16}$$

If we call α^* the contact shift angle defined in the body fixed frame and the same angle in the track reference frame, is possible to observe that $|\alpha_1^*| = |\alpha_2^*| \alpha = \gamma_0 \psi$.

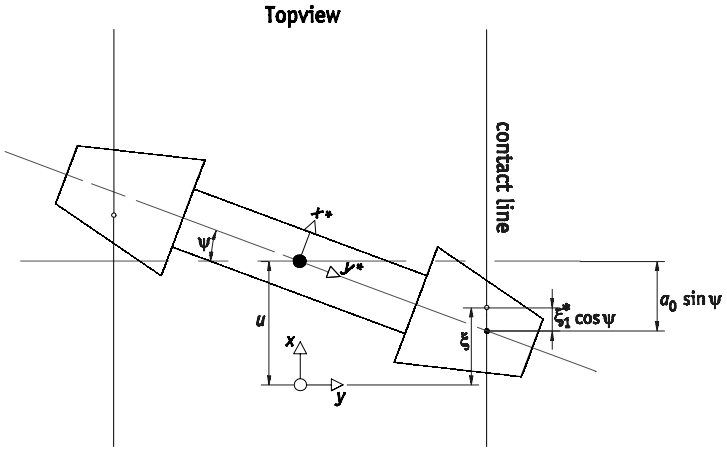

Fig. 4. The contact point shift defined in the roller-body frame (oxyz). In particular, the contact point shift at the right wheel is considered.

2.5. Wheelset on rollers

Due to the presence of the rollers instead of the rails, the expression defining the contact point shift ξ_j becomes more complex. In this case the contact point shift is affected by the curvature $1/r_r$ of the roller. Moreover, it is $\xi = \xi(u, \psi)$ because now this shift does not depend only on the yaw angle but there is a sensible influence exerted by the longitudinal displacement u of the center of mass of the wheelset o^* with respect to the roller-body frame. Then it is necessary to distinguish between the contact point shift ξ_j defined in the roller-body frame and ξ_j^* expressed in the wheelset-body frame. In order to find their definitions Fig. 4 must be considered.

This figure shows that, if only the wheelset is considered, the x coordinate of the contact point in the inertial frame reads:

$$x = u \mp a_0 \sin\psi + \xi_j^* \cos\psi \cong u \mp a_0\psi + \xi_j^*. \tag{17}$$

If we consider only the rollers, as the roller-body frame coincides with the inertial frame, we have that:

$$x = \xi_j. \tag{18}$$

As the points considered in Eqs (12) and (13) are the same, we obtain:

$$\xi_j = u \mp a_0\psi + \xi_j^* \tag{19}$$

Moreover, at the contact points, the normal vectors to the tangent surfaces must be coincident. The normal to the contact surface of the wheel, in the wheelset-body frame, is:

$$\underline{n}_j^* = [\xi_j^*/r_0 \pm \gamma_0 \; 1]^T. \tag{20}$$

The normal to the contact surface of the roller, in the roller-body frame is analogue to Eq. (20):

$$\underline{n}_j = [-\xi_j/r_r \pm (\gamma_0 \mp \varphi) \;\; 1]^T. \tag{21}$$

When transformed in the inertial frame $\underline{n}_j^*$ must be equal to $\underline{n}_j$, therefore:

$$\begin{bmatrix} 1 & -\psi & 0 \\ \psi & 1 & -\varphi \\ 0 & \varphi & 1 \end{bmatrix} \begin{bmatrix} \xi_j^*/r_0 \\ \pm\gamma_0 \\ 1 \end{bmatrix} = \begin{bmatrix} -\xi_j/r_r \\ \pm(\gamma_0 \mp \varphi) \\ 1 \end{bmatrix} \tag{22}$$

and the first of the three resulting equations yields:

$$\frac{\xi_j}{r_r} + \frac{\xi_j^*}{r_0} = \pm\gamma_0\psi. \tag{23}$$

This equation together with Eq. (19) yields:

$$\xi_j^* = \frac{r_r(-u \pm b_r\psi)}{r_r + r_0} \tag{24}$$

$$\xi_j = \frac{r_r(u \mp b_0\psi)}{r_r + r_0} \tag{25}$$

with:

$$b_r = a_0 + r_r\gamma_0, \quad b_0 = a_0 - r_0\gamma_0 \tag{26}$$

In this case, because of the effect of u, we have to define two different values of the shift angle for the two contact points A_1 and A_2. Therefore, in the wheelset-body frame we have:

$$\alpha_j^* = \frac{\xi_j^*}{r_0}, \tag{27}$$

and in the roller-body frame:

$$\alpha_j = \frac{\xi_j}{r_r} \tag{28}$$

3. Kinematics

Two types of motion are possible for the model. One is the fundamental motion in which the wheelset translates remaining in the central position. The other is the parasitic motion in which the wheelset moves about its nominal configuration. It is necessary to distinguish once more the case of wheelset running on track from the case of wheelset on rollers.

3.1. Wheelset on rails

In order to describe completely the motion of the wheelset we will take into account a transfer motion and a relative motion. The former is the motion of the track reference frame with respect to the inertial system. The latter is the motion of the wheelset relative to the track reference frame. Superimposing these two motions it is possible to obtain the total velocity of the wheelset mass center and the total angular velocity.

$$\underline{v}_0 = \underline{v}_{\mathrm{trf}} + \underline{v}_{\mathrm{rel}} \tag{29}$$

$$\underline{\omega} = \underline{\omega}_{\mathrm{trf}} + \underline{\omega}_{\mathrm{rel}} \tag{30}$$

The transfer velocity of the point o is denoted by $\vec{v}_{\mathrm{trf}}$:

$$\underline{v}_{\mathrm{trf}} = [V_n, 0, 0]^T. \tag{31}$$

The position of the point o^* with respect to the track reference frame is defined by the vector $\underline{v}_{0\mathrm{rel}}$:

$$\underline{r}_{0\mathrm{rel}} = [u, \nu, w]^t \tag{32}$$

therefore, the relative velocity of o^* is defined by:

$$\underline{v}_{\mathrm{rel}} = \dot{r}_{0\mathrm{rel}} \tag{33}$$

and consequently:

$$\underline{v}_{\mathrm{rel}} = [\dot{u}, \dot{\nu}, \dot{w}]^T, \tag{34}$$

The total velocity of the wheelset mass center, according to Eq. (29), is:

$$\underline{v}_0 = [V_0 + \dot{u}, \dot{\nu}, \dot{w}]^T, \tag{35}$$

defined with respect to the inertial frame.

The transfer angular velocity of the wheelset is denoted by $\underline{\omega}_{\mathrm{trf}}$, whereas the relative angular velocity of the same body is defined by means of the vector $\underline{\omega}_{\mathrm{rel}}$. As is the case considered here, the wheelset runs on a straight tangent track, the transfer angular velocity of the track reference frame vanishes and so, according to Eq. (30), the vector of the total angular velocity of the wheelset becomes:

$$\underline{\omega} = \underline{\omega}_{\mathrm{rel}}^{12} \tag{36}$$

where the index 12 stresses that the algebraic vector is defined with respect to the wheelset-body frame, as it is more convenient to draw up the Euler equation with respect to the body-fixed frame.

As described in Appendix A2, it is possible to reach the following compact formulation:

$$\begin{bmatrix} \underline{v}_0 \\ \underline{\omega} \end{bmatrix} = V_n[1 \quad 0 \quad 0 \quad 0 \quad -r_0^{-1} \quad 0]^T + \underline{A}\dot{\underline{q}}^*. \tag{37}$$

Another kinematic variable to be taken into account is the angular acceleration corresponding to $\underline{\omega}_{\mathrm{rel}}^{12}$. According to [13] this is given by:

$$\dot{\underline{\omega}}_{\mathrm{rel}}^{12} = \underline{H}\dot{\underline{q}}_r + \underline{h} - \ddot{\underline{\vartheta}}_n, \tag{38}$$

with:

$$\underline{h} = \begin{bmatrix} \dot{\psi}(\Omega_n - \dot{\chi}) \\ \dot{\varphi}\dot{\psi} \\ \dot{\varphi}(\dot{\chi} - \Omega_n) - \varphi\dot{\varphi}\dot{\psi} \end{bmatrix} \tag{39}$$

As the nominal angular speed is constant, the nominal angular acceleration $\ddot{\underline{\vartheta}}_n$ is equal to zero.

3.2. Wheelset on rollers

From the kinematical point of view the essential differences between the tangent track problem and the roller rig problem are caused by a different change of displacement of the wheelset mass center and by the rotation of the rollers as is clear comparing Eqs (42) and (43). In the case under examination the motion of the rollers is limited to their fundamental motion: a rotation about the spin axis with constant angular velocity $\overline{\Omega}_r$.

A simplification of the study of the kinematics of a wheelset on rollers is due to the absence of the moving track-reference frame that is here substituted by the roller-body frame $\{o, \bar{e}^1\}$, which coincides with the inertial frame. So both the transfer velocity and the transfer angular velocity are zero. It can easily deduced that:

$$\underline{v}_0 = \underline{v}_{\mathrm{rel}} \quad \underline{\omega} = \underline{\omega}_{\mathrm{rel}}. \tag{40}$$

$$\begin{aligned} &\text{As } \underline{v}_{\mathrm{rel}} = \dot{\underline{r}}_{0\mathrm{rel}} \text{ and} \\ &\quad \underline{r}_{0\mathrm{rel}} = [u \quad v \quad w]^T, \end{aligned} \tag{41}$$

we get, in the roller-body frame:

$$\underline{v}_0 = [\dot{u} \quad \dot{v} \quad \dot{w}]^T = \dot{\underline{q}}_t. \tag{42}$$

The relative angular velocity is defined in the wheelset-body frame, thus:

$$\underline{\omega} = \underline{\omega}_{\mathrm{rel}}^{21}, \tag{43}$$

where $\underline{\omega}_{\mathrm{rel}}^{21}$ is the same expressed by (A2.4). Expression Eq. (37) now become:

$$\begin{bmatrix} \underline{v}_0 \\ \underline{\omega} \end{bmatrix} = \frac{V_n}{r_0}[0 \quad 0 \quad 0 \quad 0 \quad -1 \quad 0]^T + \underline{A}\dot{\underline{q}}^* \tag{44}$$

with the matrix $\underline{A}$ defined as in (A2.8).

Finally it must be pointed out that also the angular acceleration is caused only by the relative component and so, in the wheelset-body frame, it is:

$$\dot{\underline{\omega}} = \dot{\underline{\omega}}_{\mathrm{rel}}^{12} = \underline{H}\ddot{\underline{q}}_r + \underline{h} - \ddot{\underline{\vartheta}}_n, \tag{45}$$

with $\underline{h}$ defined as in Eq. (39).

4. Creep components and spin creep

According to [14], the longitudinal and lateral creepages are given by the ratio between the relative velocity at the contact point, taken with respect to the contact frame $\{o^j, \overline{e}^{Aj}$, and the nominal velocity V_n. If the vector of the relative velocity at each contact point is denoted by $\overline{W}_{tj}$, the creep components can be defined as follows:

$$\begin{bmatrix} v_{xj} \\ v_{yj} \\ 0 \end{bmatrix} = \frac{1}{V_n} \underline{W}_{tj} \tag{46}$$

According to [13] the spin is due to the conicity of the wheel and it is given by:

$$\varphi_{sj} = \frac{1}{V_n} \omega_{nj} \tag{47}$$

Equation (46) can be simplified as shown on Appendix A3, neglecting high order terms. In case of wheelset running on track the following result has been obtained:

$$\begin{aligned} v_{xj} &= \frac{r_0 - r_j}{r_0} + \frac{\dot{u}}{V_n} + \frac{\dot{\chi}}{r_0 V_n} \mp \frac{a_j \dot{\psi}}{V_n} + O_2 \\ v_{yj} &= -\psi + \frac{1 + A_0(r_j + \gamma_0 a_j)}{V_n} \dot{v} + O_2 \\ \varphi_{sj} &= \mp \frac{\gamma_0}{r_0} + O_1. \end{aligned} \tag{48}$$

In case of wheelset on rollers a more complex equation can be obtained:

$$\begin{aligned} v_{xj} &= (r_0 - r_j) \frac{r_0 + r_r}{V_n} + \frac{\dot{u}}{V_n} + \frac{\dot{\chi}}{r_0 V_n} \mp \frac{a_j \dot{\psi}}{V_n} + O_2 \\ v_{yj} &= -\psi + \frac{1 + A_0(r_j + \gamma_0 a_j)}{V_n} \dot{v} + O_2 \\ \varphi_{sj} &= \mp \gamma_0 \left(\frac{1}{r_0} + \frac{1}{r_r} \right) + O_1. \end{aligned} \tag{49}$$

5. Dynamics

For a single rigid body such as a wheelset, the motion with respect to a non-inertial coordinate system can be determined by means of the Newton-Euler equations. The transfer angular velocity of the wheelset with respect to the inertial frame $\underline{\omega}_{\mathrm{trf}}$ is zero, according to [13] and [15], in the algebraic form, the Newton equation reads:

$$m(\underline{\dot{v}}_{\mathrm{trf}} + \underline{\dot{v}}_{\mathrm{rel}}) = \underline{f}_T \tag{50}$$

and the Euler equation:

$$\underline{I}^* \underline{\dot{\omega}}^{21}_{\mathrm{rel}} + \tilde{\underline{\omega}}^{21}_{\mathrm{rel}} \underline{I}^* \underline{\omega}^{21}_{\mathrm{rel}} = \underline{f}_R. \tag{51}$$

Here m represents the mass of the wheelset, $\underline{I}^*$ is the inertia tensor with respect to the body-fixed coordinate system (o^*, x^*, y^*, z^*) whose axes are the main inertia axes. Thus:

$$\underline{I}^* = \begin{bmatrix} I & 0 & 0 \\ 0 & I_y & 0 \\ 0 & 0 & I \end{bmatrix}. \tag{52}$$

$I = I_x = I_z$ and I_y are the wheelset moments of inertia about the principal axes of inertia.

Moreover, the symbol $\underline{f}_T$ represents the total force applied at the wheelset and the symbol the resultant moment of the applied forces. The Newton equation are taken with respect to the track-reference frame, whereas those of the

Euler equation are taken with respect to the wheelset-body frame. This simplifies the determination of the equations of motion. Taking into account Eqs (31), (34) and (A2.4), after some manipulations the Newton-Euler equations can be written in the following compact form:

$$\underline{MH^*}\,\underline{\ddot{q}} = \underline{k}_G + \underline{f} \tag{53}$$

where:

$$\underline{M} = \begin{bmatrix} m\underline{E} & \underline{O} \\ \underline{O} & \underline{I}^* \end{bmatrix}, \tag{54}$$

$\underline{k}_G$ is the vector of the gyroscopic forces:

$$\underline{k}_G = -\frac{I_y V_n}{r_0}[0 \;\; 0 \;\; 0 \;\; \dot{\psi} \;\; 0 \;\; -\dot{\varphi}]^T, \tag{55}$$

$\underline{f}$ is the vector containing the resultant forces and the resultant moments applied at the system.

$$\underline{f} = \begin{bmatrix} \underline{f}_t \\ \underline{f}_r \end{bmatrix} = \underline{k}_W + \underline{k}_T + \underline{k}_C. \tag{56}$$

$\underline{k}_W$ is the vector of the weight forces, $\underline{k}_T$ is the contribution of the tangential forces in the contact points and $\underline{k}_C$ is the contribution of the constraint forces acting on the wheelset, related with the normal forces in the contact points.

Now, in order to express the equations of motion of the system as a function of the four independent coordinates, relation Eqs (A2.12), (56) must be substituted into Eq. (53). In such a way we obtain:

$$\underline{M}(\underline{H^*}\,\underline{J})\underline{\ddot{q}}^* = \underline{k}_G + \underline{f} \Rightarrow \underline{MA}\underline{\ddot{q}}^* = \underline{k}_g + \underline{k}_W + \underline{k}_T + \underline{k}_C. \tag{57}$$

If both sides of Eq. (57) are left multiplied by $\underline{A}^T$ the matrix form of the equations of motion reads:

$$\underline{M}_A\underline{\ddot{q}}^* = \underline{k}_G + \underline{k}_W + \underline{k}_T + \underline{k}_C) \tag{58}$$

where

$$\underline{M}_A = \underline{A}^t\underline{MA}.$$

Furthermore, it can be demonstrated (See [10]) that:

$$\underline{A}^T\underline{k}_C = \underline{O}. \tag{59}$$

Equation (58) reduces to:

$$\underline{M}_A\underline{\ddot{q}}^* = \underline{A}^T(\underline{k}_G + \underline{k}_W + \underline{k}_T). \tag{60}$$

5.1. Wheelset on rails

The weight force is involved only in Newton's law, so it has to be defined in the track reference frame. Thus:

$$\underline{k}_W = [0 \;\; 0 \;\; mg \;\; 0 \;\; 0 \;\; 0]^T. \tag{61}$$

Regarding the determination of $\underline{k}_T$, it is useful to distinguish the 3×1 vector of the tangential forces $\underline{k}_{Tt}$, to be defined in the track reference frame, from the 3×1 vector of the moments they yield $\underline{k}_{Tr}$, to be defined in the wheelset-body frame:

$$\underline{k}_T = \begin{bmatrix} \underline{k}_{Tt} \\ \underline{k}_{Tr} \end{bmatrix}. \tag{62}$$

In vector form:

$$\overline{k}_{Tt} = \overline{T}_1 + \overline{T}_2 \quad \overline{k}_{Tr} = (\overline{p}_1 \times \overline{T}_1 + \overline{M}_{z1}) + (\overline{p}_2 \times \overline{T}_2 + \overline{M}_{z2}).$$

In algebraic form Eq. (62) becomes:

$$\underline{k}_T = \sum_{j=1}^{2} \left(\begin{bmatrix} \overline{G}^{1,Aj} \\ \tilde{\underline{p}}_j \underline{G}^{2,Aj} \end{bmatrix} \begin{bmatrix} T_{xj} \\ T_{yj} \\ 0 \end{bmatrix} + \begin{bmatrix} \underline{O} \\ \underline{G}^{2,Aj} \end{bmatrix} \begin{bmatrix} 0 \\ 0 \\ M_{zj} \end{bmatrix} \right) = \underline{D}_T \begin{bmatrix} T_{x1} \\ T_{x1} \\ 0 \\ T_{x2} \\ T_{x2} \\ 0 \end{bmatrix} + \underline{D}_M \begin{bmatrix} 0 \\ 0 \\ M_{z1} \\ 0 \\ 0 \\ M_{z2} \end{bmatrix}, \tag{63}$$

where $\tilde{\underline{p}}_j^*$ is the position vector defined in (A3.4), is the spin moment in the contact point and T_{xj}, T_{yj} are the resultants creep forces in longitudinal and lateral direction. These forces as well as the spin moment are applied at the contact point: the tangent forces lie in the contact plane whereas the spin moment is perpendicular to that plane. Thus all these vectors have been expressed in the contact point frame. Moreover:

$$\underline{D}_T = \begin{bmatrix} \underline{G}^{1,A1} & \underline{G}^{1,A2} \\ \tilde{\underline{p}}_1 \underline{G}^{2,A1} & \tilde{\underline{p}}_2 \underline{G}^{2,A2} \end{bmatrix} \quad \underline{D}_m = \begin{bmatrix} \underline{O} & \underline{O} \\ \underline{G}^{2,A1} & \underline{G}^{2,A2} \end{bmatrix}. \tag{64}$$

Now all the terms of the Newton-Euler Eq. (60) have been defined. After some computations it is possible to get the following set of four non-linear equations of motion:

$$\begin{aligned} &\begin{bmatrix} m & 0 & 0 & 0 \\ 0 & m + A_0^2 I & 0 & 0 \\ 0 & 0 & I_y & -A_0 I_y v \\ 0 & 0 & -A_0 I_y v & I \end{bmatrix} \begin{bmatrix} \ddot{u} \\ \ddot{v} \\ \ddot{\chi} \\ \ddot{\psi} \end{bmatrix} = \frac{I_y V_n}{r_0} \begin{bmatrix} 0 & 0 & 0 & 0 \\ 0 & 0 & 0 & A_0 \\ 0 & 0 & 0 & 0 \\ 0 & -A_0 & 0 & 0 \end{bmatrix} \begin{bmatrix} \dot{u} \\ \dot{v} \\ \dot{\chi} \\ \dot{\psi} \end{bmatrix} \\ &+ \begin{bmatrix} -2c_x & 0 & 0 & -(T_{y1} + T_{y2}) \\ 0 & -mgC_0 & 0 & (T_{x1} + T_{x2}) \\ 0 & \lambda(T_{x1} - T_{x2} & 0 & 0 \\ 0 & \lambda(T_{x1} - T_{x2}) & 0 & 0 \\ 0 & \left(\frac{\lambda}{\gamma_0} - A_0 r_0\right)(T_{x1} + T_{x2}) & 0 & (T_{y1} - T_{y2})\gamma_0 r_0 + mgD_0 \end{bmatrix} \begin{bmatrix} u \\ v \\ \chi \\ \psi \end{bmatrix} \\ &+ \begin{bmatrix} (T_{x1} + T_{x2}) \\ (T_{y1} + T_{y2})\frac{A_0 a_0}{\gamma_0} \\ (T_{x1} + T_{x2})r_0 + (M_{z1} + M_{z2})\gamma_0 \\ -(T_{x1} - T_{x2})a_0 + (M_{z1} + M_{z2}) \end{bmatrix} \end{aligned} \tag{65}$$

5.2. Wheelset on rollers

The only changes with respect to the tangent track problem are due to the different orientation of the contact plane in the space. This , as seen before, causes a different definition for the shift angle and a slightly different formulation for the rotation matrices (A1.4) and (A1.5). As a consequence, the only term in the equation of motion Eq. (60) affected by the presence of the rollers is the vector of the creep forces and moments $\underline{k}_T$. Proceeding as already seen in the above case it is possible to get the following set of non-linear differential equations of motion:

$$\begin{aligned} &\begin{bmatrix} m & 0 & 0 & 0 \\ 0 & m + A_0^2 I & 0 & 0 \\ 0 & 0 & I_y & -A_0 I_y v \\ 0 & 0 & -A_0 I_y v & I \end{bmatrix} \begin{bmatrix} \ddot{u} \\ \ddot{v} \\ \ddot{\chi} \\ \ddot{\psi} \end{bmatrix} = \frac{I_y V_n}{r_0} \begin{bmatrix} 0 & 0 & 0 & 0 \\ 0 & 0 & 0 & A_0 \\ 0 & 0 & 0 & 0 \\ 0 & -A_0 & 0 & 0 \end{bmatrix} \begin{bmatrix} \dot{u} \\ \dot{v} \\ \dot{\chi} \\ \dot{\psi} \end{bmatrix} \\ &+ \begin{bmatrix} 0 & 0 & 0 & -(T_{y1} + T_{y2}) \\ 0 & -mgC_0 & 0 & (T_{x1} + T_{x2}) \\ 0 & (T_{x1} - T_{x2})\lambda & 0 & 0 \\ -(T_{y1} + T_{y2})\frac{r_r}{r_r + r_0} & \left(\frac{\lambda}{\gamma_0} - a_0 r_r\right)(T_{x1} + T_{x2}) & 0 & (T_{y1} - T_{y2})\frac{r_r(a_0 + r_r\gamma_0)}{r_r + r_0} + mgD_0 \end{bmatrix} \begin{bmatrix} u \\ v \\ \chi \\ \psi \end{bmatrix} \end{aligned} \tag{66}$$

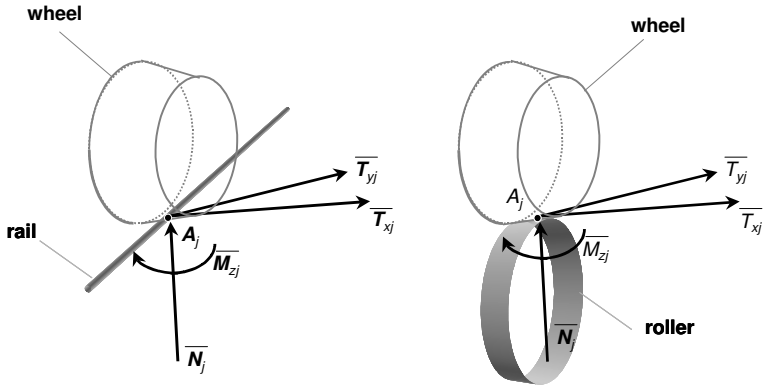

Fig. 5. Contact forces and spin moments.

$$+\begin{bmatrix} (T_{x1}+T_{x2}) \\ (T_{y1}+T_{y2})\frac{A_0 a_0}{\gamma_0} \\ (T_{x1}+T_{x2})r_0+(M_{z1}+M_{z2})\gamma_0 \\ -(T_{x1}-T_{x2})a_0+(M_{z1}+M_{z2}) \end{bmatrix}+O_2$$

According to Kalker's simplified theory [14], the creep forces T_{xj}, T_{yj} (Fig. 5), are non-linear functions of the creep quantities, of the shape of the contact area and, above all, of the constraint forces N_j (Fig. 5) applied at the wheelset body:

$$\begin{aligned} T_{xj} &= f_{xj}(\xi,\eta,\chi,a/b)\cdot\mu N_j, \\ T_{yj} &= f_{yj}(\xi,\eta,\chi,a/b)\cdot\mu N_j, \end{aligned} \tag{67}$$

The constraint forces are then implicitly involved in the equations of motion. Therefore, Eqs (65) and (66) are coupled with the constraint equations and now it is necessary to determine them.

6. Constraint equations

The vector $\underline{k}_C$ of relation Eq. (56) has to be defined. As was done for $\underline{k}_T$, it is useful to distinguish the 3×1 vector of the constraint forces applied to the wheelset $\underline{k}_{Ct}$, to be defined in the track reference frame, from the 3×1 vector of the moments they yield $\underline{k}_{Cr}$, to be defined in the wheelset-body frame:

$$\underline{k}_C = \begin{bmatrix} \underline{k}_{Ct} \\ \underline{k}_{Cr} \end{bmatrix}. \tag{68}$$

In vector form we can write:

$$\overline{k}_{Ct} = \overline{N}_1 + \overline{N}_2 \;\; \overline{k}_{Tr} = (\overline{p}_1^* \times \overline{N}_1) + (\overline{p}_2^* \times \overline{N}_2)$$

therefore, the matrix form of the formulas for the resultant constraint forces and moments applied to the wheelset reads:

$$\underline{k}_C = -\sum_{j=1}^{2}\left(\begin{bmatrix} \underline{n}_j \\ \tilde{\underline{p}}_j^* \underline{n}_j \end{bmatrix} N_j\right) = \underline{D}_N \begin{bmatrix} N_1 \\ N_2 \end{bmatrix}, \tag{69}$$

where $\underline{D}_N$ is the so-called distribution matrix of the normal contact forces N_1 and N_2:

$$\underline{D}_N = -\begin{bmatrix} \underline{n}_1 & \underline{n}_2 \\ \tilde{\underline{p}}_1^* \underline{n}_1 & \tilde{\underline{p}}_2^* \underline{n}_2^* \end{bmatrix}. \tag{70}$$

Moreover, substituting Eqs (69) into (59) it is found that now also:

$$\underline{A}^T \underline{D}_N = \underline{O}. \tag{71}$$

A method for the determination of the constraint forces $\underline{k}_C$ together with the normal forces Nj, has been described by Schielen in [16]. It consists of premultiplying the Eq. (57) by $\underline{D}_N^t \underline{M}^{-1}$. Taking into account Eq. (71):

$$\underline{D}^T \underline{M}^{-1} = (\underline{k}_g + \underline{k}_W + \underline{k}_T + \underline{k}_C) = \underline{0}. \tag{72}$$

Together with Eq. (69) it is possible to obtain the equation:

$$\underline{D}_N^T \underline{M}^{-1} \underline{D}_N \begin{bmatrix} N_1 \\ N_2 \end{bmatrix} = \underline{D}_N^T \underline{M}^{-1} (\underline{k}_G + \underline{k}_W + \underline{k}_T), \tag{73}$$

yielding the equation:

$$\begin{bmatrix} N_1 \\ N_2 \end{bmatrix} = (\underline{D}_N^T \underline{M}^{-1} \underline{D}_N)^{-1} \underline{D}_N^T \underline{M}^{-1} (\underline{k}_g + \underline{k}_W + \underline{k}_T) \tag{74}$$

by means of which, together with the Eqs (65) or (66) and (67), the six forces T_{xj}, T_{yj} and Nj can be found.

6.1. Wheelset on rails

The difference between the two systems, in this case, is due to $\underline{n}_j$ and $\underline{n}_j^*$: respectively the normal vectors of the contact plane with respect to the track reference frame and to the wheelset-body frame.

$$\underline{n}_j = [0 \quad \pm(\gamma_0 \mp \varphi) \quad 1]^T \quad \underline{n}_j^* = [\pm\alpha \quad \pm\gamma_0 \quad 1]^T.$$

For the wheelset running on a tangent track, α is given by the relation Eq. (16).

6.2. Wheelset on rollers

Here the normal vectors read:

$$\underline{n}_j^* = [\alpha_j^* \quad \pm\gamma_0 \quad 1]^T. \ \underline{n}_j [\alpha_j \quad \pm(\gamma_0 \mp \varphi) \quad 1]^T.$$

The contact shift angles are found, in this case, by means of the relations Eqs (27) and (28).

7. Linearized equations of motion

The linearized equations of motion are defined in order to compute a linear stability analysis. In order to simplify this analysis the wheelset is considered as a symmetric system running with stationary motion on its central position. From the equations of motion Eqs (65–66), and from the studies performed by Yang [5] on this subject, we can observe that the lateral parasitic motion, described by the lateral displacement vand by the yaw angle ψ, uncouples from the symmetric parasitic motion due to the longitudinal displacement u and due to the angle χ. As a consequence, it is possible to conclude that only the lateral motion must be considered in the linear equations of motion utilized to check the lateral stability of the wheelset, which is the relevant one.

For the linear stability analysis, small displacements of the wheelset from its central position are considered, with very small values of the creepages. Therefore, the creep forces can be expressed with the linear Kalker's law:

$$T_{xj} = -f_{11} \upsilon_{xj} \quad T_{yj} = -f_{22} \upsilon_{yj} - f_{23} \varphi_{sj} \quad M_{zj} = -f_{23} \upsilon_{yj} - f_{33} \varphi_{sj} \tag{75}$$

where f_{11}, f_{22}, f_{23}, f_{33} are coefficients defined by Kalker in [14] and are here considered equal for the two contact points, in other words, the different size between the right and left contact ellipses is neglected.

7.1. Wheelset on rails

It is convenient, first of all, to get simplified expressions for the creep components. Introducing the relations Eqs (10) and (11) into Eq. (15) and neglecting the contribution of the highest order terms, the creep components υ_{xj}, υ_{yj} and the spin creep φ_s reduce to:

$$\upsilon_{xj} = \mp\frac{\lambda}{r_0}v \mp \frac{a_0}{V_n}\dot{\psi} + O_2 \;\; \upsilon_{yj} = -\psi + \frac{S_0}{V_n}\dot{v} + O_2 \;\; \varphi_{sj} = \mp\frac{\gamma_0}{r_0} + O_1 \tag{76}$$

considering: $S_0 = 1 + A_0 r_0 + \gamma_0 \lambda$.

Substituting Eqs (76) in (77) and subsequently Eqs (75) in (65), according to all the assumptions made in this section and neglecting the second order terms, the linearized equations of motion become:

$$\begin{bmatrix} m + A_0^2 I & 0 \\ 0 & I_y \end{bmatrix} \begin{bmatrix} \ddot{v} \\ \ddot{\psi} \end{bmatrix} = \begin{bmatrix} -2f_{22}\frac{S_0^2}{V_n} & \frac{I_y V_n}{r_0}A_0 \\ 2f_{23}\frac{S_0}{V_n} - \frac{I_y V_n}{r_0}A_0 & -2f_{11}\frac{a_0^2}{V_n} \end{bmatrix} \begin{bmatrix} \dot{v} \\ \dot{\psi} \end{bmatrix} + \begin{bmatrix} -mgC_0 & 2f_{22}S_0 \\ -2f_{11}\frac{\lambda a_0}{r_0} & -2f_{23} + mgD_0 \end{bmatrix} \begin{bmatrix} v \\ \psi \end{bmatrix} \tag{77}$$

This set of linear differential equations enables the stability analysis in the neighborhood of the nominal state of equilibrium of the dicone.

7.2. Wheelset on rollers

Proceeding in the same way as seen before it is possible to get:

$$\upsilon_{xj} = \mp\frac{\lambda}{r_0}\frac{r_0 + r_r}{r_r}v \mp \frac{a_0}{V_n}\dot{\psi} + O_2 \;\; \upsilon_{yj} = -\psi + \frac{S_0}{V_n}\dot{v} + O_2 \;\; \varphi_{sj} = \mp\gamma_0\left(\frac{1}{r_0} + \frac{1}{r_r}\right) + O_1 \tag{78}$$

Consequently, the linearized equation of motion of a single wheelset placed on a pair of rollers become:

$$\begin{aligned} \begin{bmatrix} m + A_0^2 I & 0 \\ 0 & I \end{bmatrix} \begin{bmatrix} \ddot{v} \\ \ddot{\psi} \end{bmatrix} = & \begin{bmatrix} -2f_{22}\frac{S_0^2}{V_n} & \frac{I_y V_n}{r_0}A_0 \\ 2f_{23}\frac{S_0}{V_n} - \frac{I_y V_n}{r_0} - \frac{I_y V_n}{r_0}A_0 & -2f_{11}\frac{r_0 r_r}{r_r}\frac{a_0^2}{V_n} \end{bmatrix} \begin{bmatrix} \dot{v} \\ \dot{\psi} \end{bmatrix} \\ & + \begin{bmatrix} 0 & mgC_0 \\ -2f_{11}\frac{r_0 + r_r}{r_r}\frac{\lambda a_0}{r_0} & -2f_{23}\left(1 - \frac{a_0 + r_r\gamma_0}{r_0}\right) + mgD_0 \end{bmatrix} \begin{bmatrix} v \\ \psi \end{bmatrix} \end{aligned} \tag{79}$$

8. Analysis of the characteristics of the models

8.1. Comparison of the mathematical models

In this section the differences between the two models will be analyzed in order to predict the qualitative effects they yield.

First, it is important to point out that the curvature of the rollers $1/r_r$ causes the contact area for the roller rig to have a different shape than for the track. This affects the tangential forces in the contact point. In fact, these forces depend on the dimensions of the contact ellipse and, above all, on their ratio a/b whether they are determined by means of Kalker's linear or simplified theory [14].

With regard to the kinematical aspects, the critical differences between the tangent track and the roller rig case are found out by the comparison of the formulas for the creep components $\upsilon_{xj}, \upsilon_{yj}$, and the spin expressed respectively by Eq. (48) for the tangent track and by Eq. (49) for the roller rig.

Two important differences can be noticed:

– in the longitudinal creepage of the roller rig the first term is multiplied by $(r_0 + r_r)/r_r$. Evidently, this contribution is due to the presence of the roller: a geometric counterpart endowed with the curvature $1/r_r$. Considering that:

$$\frac{r_0 + r_r}{r_r}\frac{r_0 - r_j}{r_0} = \frac{r_0 - r_j}{r_0} + \frac{r_0 - r_j}{r_r} \tag{80}$$

it is possible to notice that the roller velocity in the contact point adds a contribution to the longitudinal creepage (the second in the right hand side of Eq. (80)), which is perfectly equivalent to the one due to the rotation of the wheel (the first in the right hand side of Eq. (80)). Also, if , as in the case of a tangent track, the additional term disappears and the first equation of Eq. (48) becomes equal to the first of Eq. (49). E.g., assuming for the wheel and roller radii the typical values they have in a full scale roller rig: $r_0 = 0.46$ m, $r_r = 0.90$ m, it is possible to observe that $(r_0 + r_r)/r_r \cong 1.51$. So the first contribution of the longitudinal creepage increases of the 51% in the case of the roller rig. This increment of v_{xj} has a strong destabilizing effect for the wheelset placed on rollers. Then, from a comparison of the simplified formulas Eqs (76) and (78) found for the wheelset on track and for the wheelset on rollers respectively:

$$v_{xj} = \mp\frac{a_0 A_0}{r_0} v \mp \frac{a_0}{V_n}\dot{\psi} + O_2 \tag{81}$$

$$v_{xj} = \mp\frac{a_0 A_0}{r_0}\frac{r_0 + r_r}{r_r} v \mp \frac{a_0}{V_n}\dot{\psi} + O_2, \tag{82}$$

it is clear that the term that increases in the roller rig is related to the lateral displacement of the wheelset. A physical explanation of this is that, due to the conicity of the wheel, the points with larger radii from the wheel axle move faster than those with smaller radii do. The same is for the rollers. Thus, when the wheelset moves laterally the peripheral velocities in the two contact points are different. In the wheel-roller contact, the presence of a rotating counterpart increases this effect with the consequent raising of the values of the opposite relative velocities. In the wheel-rail contact, this phenomenon exerts a lower influence because the rails do not give any contribution to the relative velocity in the contact plane. As will be shown, this effect causes a significant decrease of the critical speed of the wheelset when it is placed on rollers.

– About the spin φ_{sj}, from the comparison of the third of Eqs (48) and (49) results that in the roller rig there is an extra member $\mp\gamma_0/r_r$. It is due to the presence of a component of the roller angular velocity along the common normal in the contact point.

The above mentioned differences in the kinematics affect both the linear and the non-linear model. Fortunately, the discrepancies in the lateral creep φ_{sj} are all terms of the second order and so their contribution become negligible.

As far as dynamics is concerned, both the Newton-Euler equations and the constraint equations are affected by the presence of the rollers. The difference, in this case, is due to the different definition of the contact point shifts and of the correspondent angles. An explanation of their effect can be provided by comparing the definitions of the contact point shift and angle in the wheelset-body frame for the tangent track case:

$$\xi_j^* = \pm r_0 \psi \gamma_0, \quad \alpha_j^* = \pm \gamma_0 \psi \tag{83}$$

and for the roller rig:

$$\xi_j^* = \frac{r_r}{r_r + r_0}[-u \pm (a_0 + r_r\gamma_0)\psi], \quad \alpha_j^* = \frac{\xi_j^*}{r_0}. \tag{84}$$

The values of ψ and u resulting from the non-linear analyses, together with the shown formulations of α_j^*, clearly illustrate that the effect due to the yaw motion in Eq. (60) is, in general, predominant with respect to the one due to u. As already shown, for the tangent track case the two contact shift angles are equal in value and opposite in their rotation direction. In the roller rig, the two angles are still opposite in sign but they are now different in value. Then, from the comparison of Eq. (59) with (60), it is evident that, apart from the contribution of u, the coefficient that multiplies the yaw angle increases sensibly.

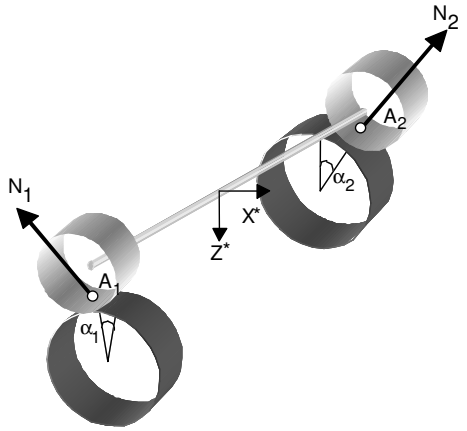

Fig. 6. The normal forces in the two contact points A1, A2 have opposite directions and different slopes. Here, in particular, $\alpha_1 > \alpha_2$.

$$\frac{(\xi_j^*)\text{ROLLER RIG}}{(\xi_j^*)\text{TG TRACK}} = \frac{r_r}{r_r + r_0}\frac{a_0 + r_r\gamma_0}{r_0\gamma_0} > 1. \tag{85}$$

This is due to the fact that in the tangent track problem the contact point shift is due uniquely to the conicity of the wheel, so if γ_0 is small the contribution of the contact shift becomes almost negligible. On the other hand, in the roller rig, the shift is also related to the hunting motion because when the contact point moves longitudinally from the centered position, the shift increases as a consequence of the curvature of the rollers. The consequence is that the two contact planes change their slopes rotating in opposite directions about the spin axis. Taking into account also the effect of the longitudinal displacement u, according to the considerations made in 2.3, the contact angles α_j become different not only for their direction but also for their value, as shown in Fig. 6.

The most relevant physical effect of these geometrical considerations finds expression in the different slope of the two normal contact forces N_1 and N_2 in the planes perpendicular to the oy axis and passing respectively through the contact points A_1 and A_2. As a consequence, the forces N_1 and N_2 yield a torque whose value, due to the presence of the rollers, is bigger than the one of the equivalent torque that is generated in the tangent track case, which is merely due to the conicity of the wheels. Therefore, the normal contact forces have, for the wheelset placed on rollers, an unstabilizing effect greater than that in the case of flat track. This effect enters the constraint Eq. (74) through the expressions of the normal vectors $\underline{n}_j^*$ and $\underline{n}_j$ which affect the distribution matrix of the normal contact forces.

8.2. Analysis of the contact patches and of their influences on the contact forces

The differences in the geometric contact between the cases of the tangent track and the roller rig affect the shape and the dimensions of the contact ellipse. In this section, these differences and their influences on the contact forces will be quantified. It will be shown, in particular, how much the discrepancies between the contact patches affect the computation of the contact forces when they are obtained by means of Kalker's linear and simplified theory (FASTSIM).

8.3. Linear model

A MATLAB program has been drawn up in order to compute the dimensions of the contact ellipse and the values of the coefficients f_{11}, f_{22}, f_{23} utilized in Eq. (75. In the following are reported the results obtained, as an example, taking into account full sized wheelset-rails and wheelset-roller systems. The values assumed for the geometrical parameters are $r_0 = 0.46$ m, $r_r = 0.90$ m, $R_r = 0.30$ m, $\gamma_0 = 0.035$ rad. The mass of the wheelset is considered to be $m = 1618$ kg.

Considering the additional contribution of the mass of bogie and car body $m_0 = 11000$ kg:

Table 1
Discrepancies between the contact coefficients involved in the linear theory. Only the wheelset mass is considered

	Tangent track	Roller rig	Percentage difference
a [mm]	3.1	2.5	−24%
b [mm]	2.4	2.5	+4%
a/b	1.3	1	−30%
f11 [kN]	$2.67 \cdot 10^3$	$2.18 \cdot 10^3$	−22%
f22 [kN]	$2.42 \cdot 10^3$	$1.91 \cdot 10^3$	−27%
f23 [kN]	2.91	1.93	−51%

Table 2
Discrepancies between the contact coefficients involved in the linear theory. In addition, the bogie mass is taken into account

	Tangent track	Roller rig	Percentage difference
a [mm]	6.1	5.0	−22%
b [mm]	4.7	5.0	+6%
a/b	1.3	1	−30%
f11 [kN]	$1.05 \cdot 10^4$	$8.58 \cdot 10^3$	−22%
f22 [kN]	$9.53 \cdot 10^3$	$7.52 \cdot 10^3$	−27%
f23 [kN]	22.66	15.03	−51%

Table 3
Discrepancies between the contact forces yielded by FASTSIM. Only the wheelset mass is considered

	Tangent track	Roller rig	Percentage difference
Tx [kN]	2.02	1.99	−1%
Ty [kN]	2.00	1.94	−3%

It can be observed, first, that in both cases the wheel-roller contact surface has a circular shape as it is shown in Fig. 7. In Tables 1 and 2 the values of the contact parameters change significantly when passing from the wheel-rail to the wheel-roller contact. In particular it can be observed that the bogie mass does not affect the percentage difference between the values of the considered parameters. Thus the discrepancy in the tangential forces generated by the wheelset when contacting the two different surfaces remains unchanged whether we consider it as a free body or connected to the bogie. In particular, as the linear creep coefficients f_{11}, f_{22}, f_{23}, are clearly much smaller in the roller rig, we may conclude that the particular wheel-roller geometric contact causes a decay of the creep forces. The direct consequence of lower creep forces is an inferior stability than in the case of tangent track.

8.4. Non-linear model

As seen before, also in this case, the tangent contact forces depend on the shape and on the dimensions of the contact area.

$$T_{xj} = f_{xj}(\xi, \eta, \chi, a/b) \cdot \mu N_j \quad T_{yj} = f_{yj}(\xi, \eta, \chi, a/b) \cdot \mu N_j.$$

These forces directly depend on a/b whereas the reduced creep components ξ, η and the reduced spin χ (See [10]) are inversely proportional to $c = ab$.

It is interesting, now, to stress again the differences deriving from the different contact patches that we find in the wheel-rail and in the wheel-roller contact.

By means of a specific MATLAB program it is possible to: analyze the characteristics of the contact patch and get the values of the tangent contact forces. Let us considering, e.g., typical values of the creepages and of the spin creep: $\upsilon_x = \upsilon_y = 2 \cdot q^{-3}$, $\varphi_s = \gamma_0(1/r_0 + 1/r_r)$. In such a way, taking into account as first the weight of the single wheelset:

Taking the same creepages and considering the influence of the bogie weight we obtain:

Obviously, the dimensions of the contact ellipses are the same as seen in the Tables 3 and 4. As was expected, the additional weight of the bogie causes an increase of the region of adhesion in the contact patch. This region, in

Table 4
Discrepancies between the contact forces yielded by FASTSIM.
The contribution of the bogie weight is taken into account

	Tangent track	Roller rig	Percentage difference
Tx [kN]	12.80	11.50	-11%
Ty [kN]	13.79	12.47	-11%

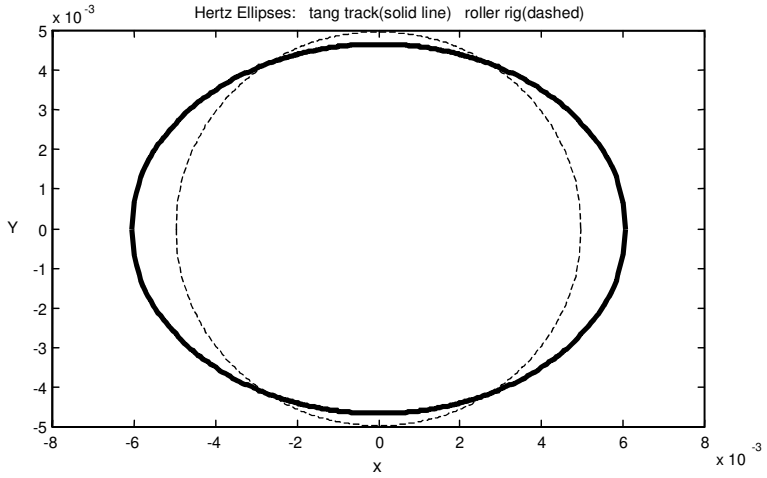

Fig. 7. Contact Ellipses determined with the contribution of the bogie mass.

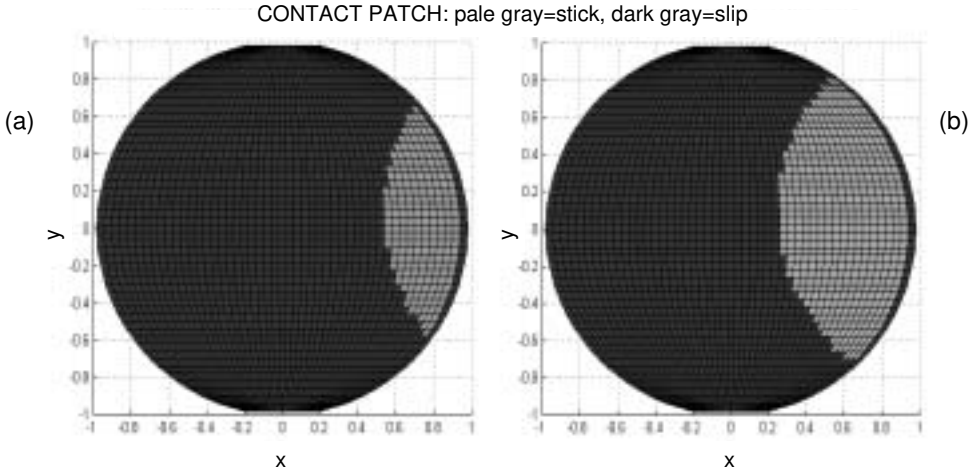

Fig. 8. Adimensionalized contact patches taken into account by FASTSIM for the computation of the tangent contact forces. Only the wheelset mass is considered; (a) Vehicle on rails; (b) vehicle on rollers.

accordance with the general results of [14], is located at the leading edge side. Unlike the linear model, the bogie weight increases the difference between the wheel-rail and the wheel-roller contact forces. However, computing the non-linear contact forces with Kalker's FASTSIM [17], the percentage differences between the forces yielded by the two kinds of contact is less evident than in the linear theory. This is due to the fact that, in the simplified theory, the adhesion area in the roller rig contact patch increases as the Figs 8 and 9 show. This effect partially compensates the negative effects due to a less extended contact patch and to a smaller ratio a/b.

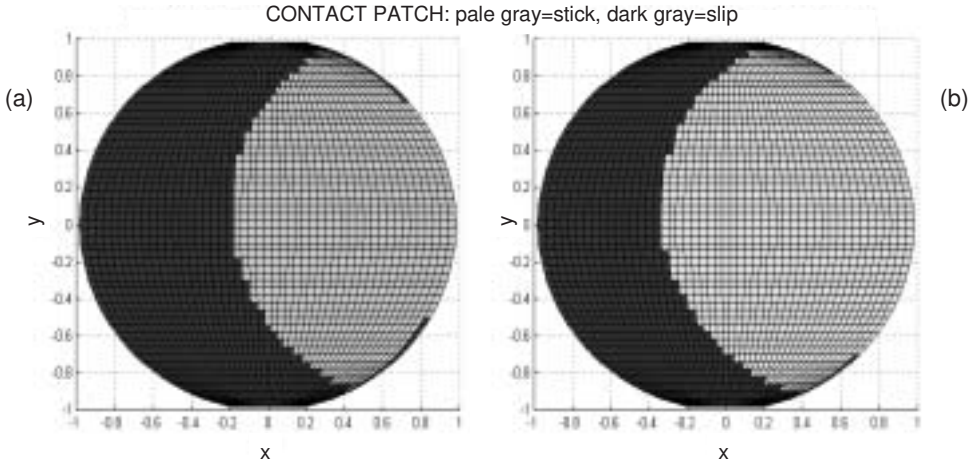

Fig. 9. Adimensionalized contact patches taken into account by FASTSIM for the computation of the tangent contact forces. The contribution of the bogie weight is taken into account. (a) Vehicle on rails; (b) vehicle on rollers.

9. Conclusions

Non linear mathematical models of wheelset on roller and track have been developed. The modeling of the dynamic and kinematics behavior of the two different systems has been developed in detail. The differences has been formally pointed out taking into account the higher order term approximations. The intrinsic differences of the two models have been put in evidence. A specific Matlab program has been developed to enhance with numerical examples the results.

It can be listed that the different behavior of the wheelset running on rails respect than on roller is mainly due to the effect of some factors:

- different shape and dimension of the contact patch;
- higher contact point shift;
- higher spin creepage;
- higher longitudinal creepage;

As a consequence the wheelset on roller is more unstable than on rails; the term which most makes unstable the wheelset is the longitudinal creepage.

List of symbols

$\{o, \overline{e}^1\}$	track reference frame
$\{o^*, \overline{e}^2\}$	wheelset-body frame
r_r	curvature radius of the rollers
r_0	nominal rolling radius of the wheelset in the central position
V_n	nominal velocity
Ω_n	nominal spin angular velocity of the wheelset
Ω_r	nominal spin angular velocity of the rollers
A_1	right contact point
A_2	left contact point
u, v, w	longitudinal, lateral, vertical traslational displacement
φ, ϑ, ψ	roll, spin and yaw angle
χ	nominal spin rotation

s	displacement of the track reference frame along the track
s^*	displacement of the wheelset-body frame
$\underline{q}^*$	vector of the independent generalized coordinates
A_0, B_0, C_0, D_0	geometrical parameters
γ_0	cone angle
a_0	wheelbase
α	shift angle
$\underline{G}_{ij}$	Rotational matrix form system i to system j
λ	equivalent conicity
$r_{1,2}$	Actual right, left rolling radius
$a_{1,2}$	Actual right, left distance of the contact point from the track center line.
R_r, R_W	Rail, Wheelset curvature radii in the x-z plane
ξ	contact point shift
$\underline{n}_j^*$	normal vector to the contact surface of the wheel in the wheelset-body frame
$\underline{n}_j$	normal vector to the contact surface of the wheel in the roller-body frame
$\underline{v}_0$	total velocity of the wheelset mass center
$\underline{\omega}$	total angular velocity
$\underline{v}_{\mathrm{trf}}$	transfer velocity of o
$\underline{r}_{0\mathrm{rel}}$	position of the point o^* respect to the track reference frame
$\underline{v}_{\mathrm{rel}}$	relative velocity of o^*
$\underline{\omega}_{\mathrm{trf}}$	transfer angular velocity of the wheelset
$\underline{\omega}_{\mathrm{rel}}$	relative angular velocity of the wheelset
J	Jacobian matrix
$\overline{W}_{ij}$	vector of the relative velocity at each contact point
ω_{nj}	component of the wheel angular velocity normal to the contact surface
$\underline{p}_j^*$	position vector of the contact point A_j in the o^* coordinate system
υ_{xj}	x creep components
υ_{yj}	y creep component
φ_{sj}	spin creep
m	mass of the wheelset
$\underline{I}^*$	*inertia tensor with respect to the body-fixed coordinate system*
$\underline{M}$	Mass matrix
$\underline{k}_G$	vector of the gyroscopic forces
$\underline{f}$	resultant vector of applied forces and moments
$\underline{k}_W$	vector of the weight forces
$\underline{k}_T$	vector of the tangential forces in the contact points
$\underline{k}_C$	constraint forces acting on the wheelset
T_{xj}, T_{yj}	creep forces
N_j	constraint forces
μ	friction coefficient
$f_{11}, f_{22}, f_{23}, f_{33}$	Kalker coefficients

Appendix A1: Transformations

The rotation matrices to pass from one coordinate system to another, are obtained by considering Tait-Bryan angles (see [13].): φ, χ, ψ and the contribution of the shift angle and of the cone angle γ_0. All these angles are assumed to be small angles, so that: $\sin(\mathrm{angle}) = \mathrm{angle}$, $\cos(\mathrm{angle}) = 1$.

The rotation matrix to pass from the body-fixed reference frame $\overline{e}^2$ to the frame $\overline{e}^1$ is obtained, first of all, rotating the system an angle φ about the x-axis with and subsequently rotating ψ an angle about the z-axis.

We obtain:

$$\underline{G}_{12} = \begin{bmatrix} 1 & -\psi & 0 \\ \psi & 1 & -\varphi \\ 0 & \varphi & 1 \end{bmatrix} \tag{A1.1}$$

Wheelset on rails

The transformation from the contact point frames $\overline{e}^{A1}$ and $\overline{e}^{A2}$ to the wheelset-body frame $\overline{e}^{2}$ is obtained rotating an angle $\pm\alpha$ about the x-axis and subsequently rotating an angle about the y-axis:

$$\underline{G}_{2,Aj} = \begin{bmatrix} 1 & 0 & \pm\alpha \\ 0 & 1 & \pm\gamma_0 \\ \mp\alpha & \mp\gamma_0 & 1 \end{bmatrix} \tag{A1.2}$$

The rotation matrices for the transformation from the contact frames $\overline{e}^{A1}$, $\overline{e}^{A2}$ to the frame $\overline{e}^{1}$ are given by the products $G_{1,Aj} = G_{12} \cdot G_{2,Aj}$:

$$\underline{G}_{1,Aj} = \begin{bmatrix} 1 & -\psi & \pm\alpha \mp \gamma_0\psi \\ \psi & 1 \pm \varphi\gamma_0 & \pm\gamma_0 - \varphi \\ \mp\alpha & \mp\gamma_0 + \varphi & 1 \pm \varphi\gamma_0 \end{bmatrix} = \begin{bmatrix} 1 & -\psi & 0 \\ \psi & 1 \pm \varphi\gamma_0 & \pm\gamma_0 - \varphi \\ \mp\alpha & \mp\gamma_0 + \varphi & 1 \pm \varphi\gamma_0 \end{bmatrix}. \tag{A1.3}$$

The matrices performing the inverse rotations: $\underline{G}_{21}$, $\underline{G}_{Aj,2}$, $\underline{G}_{Aj,1}$ are respectively the transpose of Eqs (A1.1), (A1.2) and (A1.3).

Wheelset on rollers

Because of the new definition of the shift angle α, due to the contact point shift on rollers, the rotation matrices from the contact point frames to the wheelset-body frame and to the roller-body frame become respectively:

$$\underline{G}_{2,Aj} = \begin{bmatrix} 1 & 0 & \alpha_j^* \\ 0 & 1 & \gamma_0 \\ -\alpha_j^* & -\gamma_0 & 1 \end{bmatrix} \tag{A1.4}$$

$$\underline{G}_{1,Aj} = \begin{bmatrix} 1 & -\psi & -\alpha_j^* \mp \gamma_0\psi \\ \psi & 1 \pm \varphi\gamma_0 & \pm\gamma_0 - \varphi \\ \alpha_j^* & \mp\gamma_0 + \varphi & 1 \pm \varphi\gamma_0 \end{bmatrix} = \begin{bmatrix} 1 & -\psi & \alpha_j \\ \psi & 1 \pm \varphi\gamma_0 & \pm\gamma_0 - \varphi \\ \alpha_j^* & \mp\gamma_0 + \varphi & 1 \pm \varphi\gamma_0 \end{bmatrix}. \tag{A1.5}$$

Appendix A2: Kinematics

According to [12] the angular velocity $\underline{\omega}_{\mathrm{rel}}^{12}$ is given by:

$$\underline{\omega}_{\mathrm{rel}}^{12} = \underline{H}\underline{\dot{q}}_r + \underline{\dot{\vartheta}_n} \tag{A2.1}$$

where, assuming φ as a small angle:

$$\underline{H} = \begin{bmatrix} 1\,0\,0 \\ 0\,1\,\varphi \\ 0\,0\,1 \end{bmatrix} \tag{A2.2}$$

and

$$\underline{\dot{q}}_r = [\dot{\varphi}, \dot{\chi}, \dot{\psi}]^T \;\; \underline{\dot{\vartheta}}_n = [0, \Omega_n, 0]^T. \tag{A2.3}$$

Therefore we get:

$$\underline{\omega} = \underline{\omega}_{\mathrm{rel}}^{12} = \begin{bmatrix} \dot{\varphi} \\ \dot{\psi}\varphi + \dot{\chi} - \Omega_n \\ \dot{\psi} \end{bmatrix}. \tag{A2.4}$$

Combining Eq. (35) with Eq. (A2.4), we obtain:

$$\begin{bmatrix} \underline{v}_0 \\ \underline{\omega} \end{bmatrix} = \begin{bmatrix} V_n + \dot{u} \\ \dot{v} \\ \dot{w} \\ \dot{\phi} \\ \dot{\chi} - \Omega_n + \varphi\dot{\psi} \\ \dot{\psi} \end{bmatrix}. \tag{A2.5}$$

The differentiation of Eqs (7) and (8) with respect to time gives:

$$\dot{\phi} = -A_0\dot{v} \tag{A2.6}$$

$$\dot{w} = -C_0 v\dot{v} + D_0\psi\dot{\psi} \tag{A2.7}$$

By means of Eqs (A2.6) and (A2.7) it is possible to eliminate the derivatives of the dependent generalized coordinates and to obtain:

$$\begin{bmatrix} \underline{v}_0 \\ \underline{\omega} \end{bmatrix} = V_n[1 \;\; 0 \;\; 0 \;\; 0 \;\; -r_0^{-1} \;\; 0]^T + \underline{A}\dot{\underline{q}}^*. \tag{3.9}$$

The matrix $\underline{A}$:

$$\underline{A} = \begin{bmatrix} 1 & 0 & 0 & 0 \\ 0 & 1 & 0 & 0 \\ 0 & -C_0 v & 0 & D_0\psi \\ 0 & -A_0 & 0 & 0 \\ 0 & 0 & 1 & -A_0 v \\ 0 & 0 & 0 & 1 \end{bmatrix} \tag{A2.8}$$

is defined by the relation:

$$\underline{A} = \underline{H}^* \cdot \underline{J} \tag{A2.9}$$

where $\underline{H}^*$ is:

$$\underline{H}^* = \begin{bmatrix} \underline{E} & \underline{O} \\ \underline{O} & \underline{H} \end{bmatrix} \tag{A2.10}$$

and J is the Jacobian matrix:

$$\underline{J} = \begin{bmatrix} 1 & 0 & 0 & 0 \\ 0 & 1 & 0 & 0 \\ 0 & \frac{\partial w}{\partial v} & 0 & \frac{\partial w}{\partial \psi} \\ 0 & \frac{\partial \varphi}{\partial v} & 0 & \frac{\partial \varphi}{\partial \psi} \\ 0 & 0 & 1 & 0 \\ 0 & 0 & 0 & 1 \end{bmatrix}, \Rightarrow \underline{J} = \begin{bmatrix} 1 & 0 & 0 & 0 \\ 0 & 1 & 0 & 0 \\ 0 & -C_0 c & 0 & D_0\psi \\ 0 & -A_0 & 0 & 0 \\ 0 & 0 & 1 & 0 \\ 0 & 0 & 0 & 1 \end{bmatrix}. \tag{A2.11}$$

It is evident that:

$$\ddot{\underline{q}} = \underline{J}\ddot{\underline{q}}^* \tag{A2.12}$$

Appendix A3: Creep components determination

Wheelset on rails

In the present work the track is assumed to be rigid, therefore, in the wheel contact point A_j the rail velocity is zero and the relative velocity $\overline{v}_j$ of the wheel with respect to the rail is simply equal to the velocity of the wheelset in the contact point. It is more convenient to define the wheelset velocity at the contact point in the wheelset-body frame and then to perform the transformation into the contact frame $\{O^j, \overline{e}^{Aj}\}$ by using the rotation matrix $\underline{G}^{Aj,2}$ obtained as indicated in appendix A1. When the velocity $\overline{v}_j$ expressed in the wheelset-body coordinate system (o^*, x^*, y^*, z^*) is denoted by , the vector $\overline{v}_j^{21}$ in algebraic form reads:

$$\underline{W}_{tj} = \underline{G}^{Aj,2} \cdot \underline{v}_j^{21} \tag{A3.1}$$

and Eq. (46) becomes:

$$\begin{bmatrix} v_{xj} \\ v_{yj} \\ 0 \end{bmatrix} = \frac{1}{V_n} \underline{G}^{Aj,2} \cdot \underline{v}_j^{21}, \tag{A3.2}$$

with:

$$\underline{v}_j^{21} = \underline{G}^{21} \underline{v}_{\mathrm{trf}} + \underline{G}^{21} \underline{v}_{\mathrm{rel}} + \tilde{\underline{\omega}}_{\mathrm{rel}}^{21} \underline{p}_j^*. \tag{A3.3}$$

where $\underline{p}_j^*$ is the vector that defines the position of the contact point A_j in the coordinate system (o^*, x^*, y^*, z^*) and turns out to be equal to:

$$\underline{p}_j^* = [\pm \alpha r_j, \pm a_j, r_j]^T. \tag{A3.4}$$

The first two terms of the right hand side of Eq. (A3.3) represent the total velocity of the wheelset defined in the wheelset-body frame:

$$\underline{v}_0^{21} = \underline{G}^{21}(\underline{v}_{\mathrm{trf}}) + \underline{v}_{\mathrm{rel}}) = \underline{G}^{21} \underline{v}_0 = \begin{bmatrix} \dot{u} + V_n + \psi \dot{v} \\ \dot{v} - \varphi(V_n + \dot{u}) \\ -\varphi \dot{v} + \dot{w} \end{bmatrix}, \tag{A3.5}$$

for the last term we have:

$$\tilde{\underline{\omega}}_{\mathrm{rel}}^{21} p_j^* = \begin{bmatrix} r_j \dot{\chi} - \Omega_n r_j \mp a_j \dot{\psi} + r_j \varphi \dot{\psi} \\ -r_j \dot{\varphi} \pm \alpha r_j \dot{\psi} \\ \pm a_j \dot{\varphi} \mp \alpha r_j \dot{\chi} \pm \alpha r_j \Omega_n \mp \alpha r_j \varphi \dot{\psi} \end{bmatrix} \tag{A3.6}$$

Neglecting the second order terms we can obtain from Eq. (A3.3):

$$\underline{v}_j^{21} = \begin{bmatrix} \dot{u} + V_n + r_j \dot{\chi} - r_j \Omega_n \mp a_j \dot{\psi} \\ \dot{v} - \psi V_n - r_j \dot{\varphi} \\ \pm a_j \dot{\varphi} \pm \alpha r_j \Omega_n \end{bmatrix} + O_2 \tag{A3.7}$$

Now, from Eq. (A3.1), it is possible to determine the velocity in the contact frame:

$$\underline{W}_{tj} = \begin{bmatrix} \dot{u} + V_n + r_j \dot{\chi} - r_j \Omega_n \mp a_j \dot{\psi} \\ \dot{v} - \psi V_n - r_j \dot{\varphi} - a_j \gamma_0 \dot{\varphi} \\ \pm \gamma_0 \dot{v} \pm (a_j - \gamma_0 r_j) \dot{\varphi}) \end{bmatrix} + O_2 \tag{A3.8}$$

It can be expressed as a function of the nominal longitudinal speed and of the independent generalized coordinates:

$$\begin{bmatrix} W_{txj} \\ W_{tyj} \\ W_{nj} \end{bmatrix} = V_n \begin{bmatrix} \frac{r_0 - r_j}{r_0} \\ -\psi \\ 0 \end{bmatrix} + \begin{bmatrix} 1 & 0 & r_j & \mp a_j \\ 0 & 1 + A_0(r_j + \gamma_0 a_j) & 0 & 0 \\ 0 & 0 & 0 & 0 \end{bmatrix} \dot{q}^* + O_2 \tag{A3.9}$$

The component in the normal direction is zero as it was expected.

In order to determine the component needed to compute the spin creepage it is now necessary to compute the angular velocity ω_{nj}:

$$[\omega_{txj} \;\; \omega_{tyj} \;\; \omega_{nj}]^T = \underline{G}^{Aj,2}\underline{\omega}_{\mathrm{rel}}^{21}, \tag{A3.10}$$

together with Eq. (A2.4) it is possible to determine:

$$\omega_{nj} = \mp\Omega_n\gamma_0 + \dot{\psi} + O_2. \tag{A3.11}$$

While the components of $\underline{W}_t$ are all quantities of order one, ω_{nj} is of order zero because of the first term of the right hand side. Thus, the first-order term in Eq. (A3.11) can be neglected. Consequently:

$$\omega_{nj} = \mp\Omega_n\gamma_0 + O_1 \tag{A3.12}$$

Finally, by means of Eqs (46), (47), (A3.9) and (A3.10), it is possible to find the creep components and the spin creep:

$$\begin{aligned} \upsilon_{xj} &= \frac{r_0 - r_j}{r_0} + \frac{\dot{u}}{V_n} + \frac{\dot{\chi}}{r_0 V_n} \mp \frac{a_j\dot{\psi}}{V_n} + O_2 \\ \upsilon_{yj} &= -\psi + \frac{1 + A_0(r_j + \gamma_0 a_j)}{V_n}\dot{v} + O_2 \\ \varphi_{sj} &= \mp\frac{\gamma_0}{r_0} + O_1. \end{aligned} \tag{4.3}$$

Wheelset on rollers

For the determination of the creepages in the roller rig, the velocities $\underline{\upsilon}_{rj}$ of the two rollers at the contact points must be taken into account. The relative velocities in the contact points: $\underline{W}_{tj}$, are given by the difference between the velocity of the wheels and the rollers in these points:

$$\underline{W}_{tj} = \underline{\upsilon}_j - \underline{\upsilon}_{rj} \tag{A3.14}$$

The definition of the velocity of the wheelset in the contact frame is given by:

$$\underline{\upsilon}_j = \underline{G}^{Aj,2} \cdot \underline{\upsilon}_j^{21} \tag{A3.15}$$

with:

$$\underline{\upsilon}_j^{21} = \underline{G}^{21}\underline{\upsilon}_0 + \tilde{\underline{\omega}}_{\mathrm{rel}}^{21}\underline{p}_j^*. \tag{A3.16}$$

$\underline{p}_j^*$ is the position vector of the contact point A_j in the coordinate system (o^*, x^*, y^*, z^*) and turns out to be equal to:

$$\underline{p}_j^* = [\xi_j^* \pm a_j, r_j]^T. \tag{A3.17}$$

The first term of the right hand side of Eq. (A3.16) yields the total velocity of the wheelset defined in the wheelset-body frame:

$$\underline{V}_0^{21} = \underline{G}^{21}\underline{\upsilon}_0 = \begin{bmatrix} \dot{u} + \psi\dot{v} \\ \dot{v} - \varphi\dot{u} \\ \dot{w} - \varphi\dot{v} \end{bmatrix}, \tag{A3.18}$$

the term related to the angular velocity becomes:

$$\tilde{\underline{\omega}}_{\mathrm{rel}}^{21}p_j^* = \begin{bmatrix} r_j\dot{\chi} - \Omega_n r_j \mp a_j\dot{\psi} + r_j\varphi\dot{\psi} \\ -r_j\dot{\varphi} + \xi_j^* r_j\dot{\psi} \\ \pm a_j\dot{\varphi} - \xi_j^*(\dot{\chi} - \Omega_n) - \xi_j^*\varphi\dot{\psi} \end{bmatrix} \tag{A3.19}$$

Neglecting the second order terms, the algebraic vector Eq. (A3.16), is hence defined as follows:

$$\underline{v}_j^{21} = \begin{bmatrix} \dot{u} + r_j\dot{\chi} - r_j\Omega_n \mp a_j\dot{\psi} \\ \dot{v} - r_j\dot{\varphi} \\ \pm a_j\dot{\varphi} + \xi_j^*\Omega_n \end{bmatrix} + O_2. \tag{A3.20}$$

Taking into account Eq. (A2.6) it is possible to write the expression of the velocity in the contact frame as a function of the nominal equivalent speed V_n and of the independent generalized coordinates:

$$\underline{v}_j = \begin{bmatrix} \dot{u} + r_j\dot{\chi} - r_j\frac{V_n}{r_0} \mp a_j\dot{\psi} + a_j^*\xi_j^*\frac{V_n}{r_0} \\ \dot{v} + A_0 r_j\dot{v} + A_0 a_j\gamma_0\dot{v} + \gamma_0\xi_j^*\frac{V_n}{r_0} \\ 0 \end{bmatrix} + O_2 \tag{A3.21}$$

The velocity $\underline{v}_{rj}$ of the roller at the contact point A_j must be now evaluated. In the absence of the parasitic motion of the rollers it is possible to calculate $\underline{v}_{rj}$ as proposed by De Pater in [15]. We introduce the vectors $\underline{p}_{rj}^0$, $\underline{v}_r^0$ and $\underline{\omega}_r$ all with Q_{0j} as the origin and defined in the roller-body frame. Then, in analogy with Eq. (A3.15) we can find $\underline{v}_{rj}$ as:

$$\underline{v}_{rj} = \underline{G}^{Aj,1}(\underline{v}_r^0 + \tilde{\underline{\omega}}_r\underline{p}_{rj}^0), \tag{A3.22}$$

with:

$$\underline{v}_r^0 = 0, \quad \underline{\omega}_r = [0 \;\; \Omega_r \;\; 0]^T. \tag{A3.23}$$

The vector $\underline{p}_{rj}^0$ is given by:

$$\underline{p}_{rj}^0 = [\xi_j \;\; \pm(a_j - a_0) \;\; r_j - (r_r + r_0)]^T. \tag{A3.24}$$

Equations (A3.22) and (A3.24) yield:

$$\tilde{\underline{\omega}}_r\underline{p}_{rj}^0 = V_n \begin{bmatrix} \frac{r_j - r_0}{r_r} - 1 \\ 0 \\ -\frac{\xi_i}{r_r} \end{bmatrix}. \tag{A3.25}$$

Now, by using of Eq. (A3.22), it is possible to obtain the expression of the roller velocities in the contact planes:

$$\underline{v}_{rj} = V_n \begin{bmatrix} \frac{r_j - r_0}{r_r} - 1 - \alpha_j^2 \\ \left(\frac{r_j - r_0}{r_r} - 1\right)\psi \pm \gamma_0\alpha_j \\ -\alpha_j^* - \alpha_j \end{bmatrix}. \tag{A3.26}$$

Substituting Eqs (A3.21) and (A3.26) into (A3.14), and omitting the second order terms, the relative velocities in the contact points become:

$$\begin{bmatrix} W_{txj} \\ W_{tyj} \\ W_{nj} \end{bmatrix} = V_n \begin{bmatrix} (r_0 - r_j)\frac{r_0 + r_r}{r_0 r_r} \\ \psi \\ 0 \end{bmatrix} + \begin{bmatrix} 1 & 0 & r_j & \mp a_j \\ 0 & 1 + A_0(r_j + \gamma_0 a_j) & 0 & 0 \\ 0 & 0 & 0 & 0 \end{bmatrix} \dot{q}^* + O_2 \tag{A3.27}$$

Then, in this case, the angular velocity ω_{nj} necessary to compute the spin creep reads:

$$\omega_{nj} = \underline{n}_j^{*T}\underline{\omega}_{\mathrm{rel}}^{21} - \underline{n}_j^T\underline{\omega}_r, \tag{A3.28}$$

and together with Eqs (2.15), (2.20) and (2.21) it is possible to determine:

$$\omega_{nj} = \mp\gamma_0\left(\frac{1}{r_0} + \frac{1}{r_r}\right) + O_1. \tag{A3.29}$$

It is now possible to determine the creep components and the spin creep:

$$\begin{aligned} v_{xj} &= (r_0 - r_j)\frac{r_0 + r_r}{r_0 r_r} + \frac{\dot{u}}{V_n} + \frac{\dot{\chi}}{r_0 V_0} \mp \frac{a_j\dot{\psi}}{V_n} + O_2 \\ v_{yj} &= -\psi + \frac{1 + A_0(r_j + \gamma_0 a_j)}{V_n}\dot{v} + O_2 \\ \varphi_{sj} &= \mp\gamma_0\left(\frac{1}{r_0} + \frac{1}{r_r}\right) + O_1. \end{aligned} \tag{4.4}$$

References

[1] R.V. Dukkipaty, Dynamics of a wheelset on roller rig, *Vehicle System Dynamics* **29** (1998).
[2] P.D. Allen and S.D. Iwnicky, The critical speed of a railway vehicle on a roller rig, *Proc Instn Mech Engrs* **214**(Part F) (2000).
[3] A. Jaschinski, *On the application of similarity laws to a scaled railway bogie model*, Köln, DLR-FB 90-06, 1990.
[4] N. Bosso, A. Gugliotta and A. Somà, *Progettazione di un banco prova in scala 1/5 per analisi sperimentale di carrelli ferroviari*, Atti del XXIX convegno AIAS. Lucca. 2000.
[5] N. Bosso, A. Gugliotta and A. Somà, *Introduction of a wheel-rail and wheel-roller contact model in a Multibody code*, ASME & IEEE Joint Rail Conference. Washington, DC, 2002.
[6] N. Bosso, A. Gugliotta and A. Somà, *Comparison of different scaling techniques for the dynamic of a bogie on roller rig.17th IAVSD Symposium*, Copenaghen (Lyngby), 2001.
[7] A. Jaschinski, H. Chollet, S.D. Iwnicki, A.H. Wickens and J. Von Würzen, The application of roller rigs to a railway vehicle dynamics, *Vehicle System Dynamics* **31** (1999), 345–392.
[8] G. Yang, *Dynamic analysis of railway wheelsets and complete vehicle systems*, Ph.D. Thesis Delft University of Technology, 1993.
[9] L. Mauer, *Die modulare beschreibung des rad/schiene-kontakts im linearen mehrkörperformalismus*, Dissertation TU-Berlin, 1988.
[10] A.D.de. Pater, P. Meijers and I.V. Shevtsov, *Simulation of the motion of a railway vehicle along curved tacks*, Delft University of Technology, Report No. 1196, 1999.
[11] A.D.de. Pater, *The motion of a railway wheelset supported by a pair of rollers as compared with the motion of such a wheelset along a tangent track*, Delft University of Technology, Report, 1993, pp. 1012.
[12] A.D.de. Pater, The geometrical contact between track and wheelset, *Vehicle System Dynamics* **17** (1988), 127–140.
[13] R.E. Roberson and R. Schwertassek, *Dynamics of multibody systems*, Berlin Heidelberg, Springer-Verlag, 1988.
[14] J.J. Kalker, *Three-dimensional elastic bodies in rolling contact*, Dordrecht, Kluwer Academic Publishers, 1990.
[15] A.D.de. Pater, *The equations of motion of a simplified railway vehicle moving along a curved track and the simulation of an uneven tangent railway track by means of a roller rig*, Delft University of Technology, Report, 1997, pp. 1058.
[16] W. Schielen, *Generalized constraint forces in ordinary multibody systems*, Proc. 14th Yugoslav Congress on Rational and Applied Mechanics, C3-16, Jugoslavensko Drustva za Mehanika, Beograd, 1978, pp. 301–308.
[17] J.J. Kalker, A fast algorithm for the simplified theory of rolling contact, *Vehicle System Dynamics* **11** (1982), 1–13.